

A POSITIONAL PFEM FORMULATION FOR SOLVING FREE SURFACE FLOW AND FSI PROBLEMS

Péricles Rafael Pavão Carvalho
Rodolfo A. K. Sanches
giavancini@usp.br
periclescarvalho@usp.br
rodolfo.sanches@usp.br
University of São Paulo

Av. Trabalhador Sãocarlense 400, 13566-590, São Paulo, Brazil

Giovane Avancini

Abstract. There are two mainly used approaches for coupling solid and fluid, the moving mesh and nonmoving mesh methods. In the first approach, arbitrary Lagrangian-Eulerian or space-time methods are employed to allow fluid mesh to deform and follow the moving structure, however such methods are not able to handle directly problems with very large displacements causing topology changes (TC) in the flow domain, like waves breaking over structures. In the second approach, immersed-boundary methods are used to allow the structure to move over a mesh that is not following the interface, being a practical way in flow problems with TC, however, it might involve numerical problems due to the conditions imposed at the immersed boundary. A more recent alternative is the particle-finite element method (PFEM), associating a Lagrangian finite element modeling of the fluid to particle method. The positional finite element method, developed in the same academic environment where this project is proposed, uses a total Lagrangian framework and naturally includes the geometric non linearity effects due to the use of nodal positions as main variables instead of displacements. Such formulation seems ideal for association with particle concepts, considering particle positions as main variables. Thus, we propose to model the fluid also using a Lagrangian framework by considering it as a set of particles which interaction forces are computed through positional finite element method each time step. To make it possible, a new mesh must be periodically constructed based on particles positions and the Lagrangian reference must be updated. Finally, a Dirichlet-Neumann coupling scheme can be employed with no need of extra techniques since the motion of both fluid and solid domain is described by means of a Lagrangian reference.

Keywords: Fluid-structure interaction, Free surface flow, Particle finite element method, Positional finite element method.



1 Introduction

Fluid-structure interaction (FSI) problems are known to be very complex as they involve two different physical domains, which imposes a lot of difficulties when solving it through a numerical approach like the Finite Element Method (FEM).

Commonly, the governing equations of fluid dynamics are described using an Eulerian reference with fixed mesh, while a Lagrangian description is employed to represent the structure motion with a deforming mesh, making hard to couple both domains as the mathematical descriptions are not compatible. To overcome this issue when using this approach, there are basically two classes of methods for coupling fluid and structure: fitted mesh and unfitted mesh methods.

Fitted mesh methods consist of applying a mesh moving technique to allow the fluid boundaries to adapt to the structure motion. In this group lies the well known Arbitrary Lagrangian Eulerian description (ALE) proposed by Donea et al. [1], widely used in coupled problems (Fernandes et al. [2], Hughes et al. [3], Del Pin et al. [4]) and the Space-Time Finite Element (DSD/SST) (Takizawa and Tezduyar [5], Masud and Hughes [6], Hübner et al. [7]).

In unfitted mesh methods, the moving boundary is immersed in a fixed spatial mesh, and the interface conditions are considered in the mathematical system as extra constrains by means of immersed boundaries (Peskin [8], Mittal and Iaccarino [9]).

Both approaches have led to significant advances in numerical simulation of free surface flows and FSI problems, however the fitted mesh methods are unable to deal directly with topological changes in the fluid domain, while immersed boundary methods present some numerical difficulties in the imposition of immersed boundary conditions and also to track the interface position inside the fluid mesh. In this sense, some numerical methods which are based on a Lagrangian description started to emerge in order to facilitate the analysis of problems which present large distortions, like the SPH (Smoothed Particle Hydrodynamics), proposed by Gingold and Monaghan [10].

Following the idea, Idelsohn et al. [11] developed a new method called Particle Finite Element Method (PFEM) using a Lagrangian reference to described the fluid motion by considering it a set of particles, eliminating the convective terms at the sime time naturally accounting for the domain distortion. It combines the traditional FEM with some techniques to identify the external boundaries and to build a new mesh over time, making possible to simulate problems like slosh of high amplitudes, water drops and breaking waves. For more applications of the PFEM, the readers can refer to Idelsohn et al. [12, 13], Oñate et al. [14], Carbonell et al. [15], Cremonesi et al. [16], Cerquaglia et al. [17].

Like in the standard FEM formulations for fluid dynamics, the traditional PFEM uses velocity as main variables when dealing with fluid dynamics due to the fact that, for Newtonian fluids, deviatoric stresses depends on strain rates. As a consequence, a numerical time integrator is needed in order to update the particles position at the end of a time step. We propose to use an alternative formulation in which the current particle positions are the main variables. The α -shape technique (Edelsbrunner and Mücke [18]) is employed to identify the external boundaries and a Delaunay triangulation is performed over time to build a new FEM mesh in order to calculate the interaction forces between particles.

The positional finite element formulation was developed in the context of solid mechanics, and it has proved to be stable and very robust for non-linear static and dynamic analyses (Greco and Coda [19], Coda and Paccola [20], Siqueira and Coda [21], Sanches and Coda [22]). By considering current positions as nodal parameters instead of displacements, it naturally includes the geometric non-linearity effects thanks to the way that positions are mapped to the reference and current configurations, using a Total Lagrangian description.

In this work we present a 2D solver for FSI problems, where large domain distortions, topological changes and geometric non-linearity are contemplated. Stabilized triangular elements with linear interpolations for positions and pressure are used for discretizing the fluid domain, while a triangular element with cubic shape functions is employed for the structural non-linear dynamic analysis. In both domains the solution in time is achieved by means of Newmark- β implicit algorithm.

Since the proposed formulation uses a Lagrangian description for both fluid and structure, it be-

comes straightforward to solve the coupled problem with no need of extra techniques. We use then a strong partitioned scheme based on a block-iterative.

2 Incompressible fluid flow problem

Let us consider that a fluid particle has its initial position denoted by \mathbf{x} at a time t_0 , and that \mathbf{y} represents its current position at time t, which is moving with a given velocity $\dot{\mathbf{y}}(\mathbf{y},t)$. With $\boldsymbol{\sigma}$ and \mathbf{b} denoting Cauchy stress tensor and body forces, respectively, the governing equations of an incompressible fluid flow are written in its Lagrangian form in the current position \mathbf{y} as:

$$\rho \frac{D\dot{\mathbf{y}}}{Dt} - \nabla \cdot \boldsymbol{\sigma} - \mathbf{b} = 0, \tag{1}$$

$$\nabla \cdot \dot{\mathbf{y}} = 0, \tag{2}$$

with velocity computed as $\dot{\mathbf{y}} = \partial \mathbf{y}/\partial t$ and $D(\cdot)/Dt$ representing the material time derivative. The problem is completed imposing the Dirichlet and Neumann boundary conditions:

$$\mathbf{y} = \overline{\mathbf{y}} \quad \text{on } \Gamma_d,$$
 (3)

$$\sigma \cdot \mathbf{n} = \mathbf{h} \quad \text{on } \Gamma_n, \tag{4}$$

where \overline{y} are prescribed positions, h denotes surface tractions, n the normal vector to the boundary and $\Gamma = \Gamma_d \cup \Gamma_n$.

For Newtonian incompressible flows, the constitutive law is defined by:

$$\sigma = 2\mu \dot{\epsilon} - pI,\tag{5}$$

in which μ is the fluid viscosity, p stands for hidrostatic pressure, I represents identity tensor and $\dot{\boldsymbol{\epsilon}}$ is the strain rate tensor, computed as $\dot{\boldsymbol{\epsilon}} = \frac{1}{2} \left(\nabla \dot{\mathbf{y}} + \nabla \dot{\mathbf{y}}^t \right)$. Substituting Equation (5) in (1) one derives the Lagrangian Navier-Stokes equations for an incompressible flow in the current configuration:

$$\rho \frac{D\dot{\mathbf{y}}}{Dt} - \mu \nabla^2 \dot{\mathbf{y}} + \nabla p - \mathbf{b} = \mathbf{0},\tag{6}$$

$$\nabla \cdot \dot{\mathbf{y}} = 0. \tag{7}$$

2.1 Spatial discretization and pressure stabilization

The weak form of Equations (6) and (7) is obtained using the classic Galerking method, so multiplying them by appropriated test functions \mathbf{w}^h and q^h , applying the divergence theorem and integrating over the current domain one has:

$$\int_{\Omega} \rho \mathbf{w}^h \cdot \ddot{\mathbf{y}}^h d\Omega + \int_{\Omega} \nabla \mathbf{w}^h \mu \nabla \dot{\mathbf{y}}^h d\Omega - \int_{\Omega} \mathbf{w}^h \nabla p^h d\Omega - \int_{\Omega} \mathbf{w}^h \cdot \mathbf{b}^h d\Omega - \int_{\Gamma} \mathbf{w}^h \cdot \mathbf{h}^h d\Gamma = \mathbf{0}, \quad (8)$$

$$\int_{\Omega} q^h \nabla \cdot \dot{\mathbf{y}}^h d\Omega = 0, \tag{9}$$

where for simplicity we named $\ddot{\mathbf{y}} = D\dot{\mathbf{y}}/Dt$. Notice that Eq. (8) is defined over current configuration, which is unknown. However, in the same way as in the velocity-based PFEM Idelsohn et al. [11], Oñate et al. [14], a good convergence is achieved by lagging the update of the integration domain in the Newton-Raphson procedure.

When dealing with free surface flows using the PFEM, it becomes necessary to approximate both position and pressure with linear shape functions in order to make easier the remesh procedure over time. Thus one has:

$$\mathbf{y}^h = N_a \mathbf{y}_a \quad \text{and} \quad p^h = N_a p_a, \tag{10}$$

in which superindex h indicates the interpolated variable over the discretized domain, N_a , y_a and p_a are the shape function, position vector and pressure related to node a. This choice of shape functions (linear for both variables) is known for violating the LBB condition and presenting pressure oscilations. For this reason we use the PSPG technique proposed by Tezduyar et al. [23], Tezduyar and Osawa [24] to stabilize the formulation. The method consists on adding to Equation (9) the momentum residual times stabilizing terms scaled by a parameter τ_{PSPG} :

$$\int_{\Omega} q^{h} \nabla \cdot \dot{\mathbf{y}}^{h} d\Omega + \sum_{e=1}^{n_{e}} \int_{\Omega_{e}} \tau_{PSPG}^{e} \frac{\nabla q^{h}}{\rho} \cdot \left(\rho \ddot{\mathbf{y}}^{h} - \nabla \cdot \boldsymbol{\sigma}^{h} - \mathbf{b} \right) d\Omega_{e} = 0, \tag{11}$$

and the stabilization parameter is computed according to Tezduyar et al. [23]. For linear elements, the viscosity term coming from $\nabla \cdot \sigma$ vanishes as it involves second order derivatives. Also, one can notice that the method is consistent since momentum residual is zero at equilibrium, thus recovering the incompressibility condition.

2.2 Time integration

Considering that t and $t + \Delta t$ refer to the previous and current time step respectively, the time integration is performed using the implicit-second order Newmark- β scheme, which approximates velocity and acceleration as:

$$\dot{\mathbf{y}}_{t+\Delta t} = \gamma \Delta t \ddot{\mathbf{y}}_{t+\Delta t} + \mathbf{r}_t, \tag{12}$$

$$\ddot{\mathbf{y}}_{t+\Delta t} = \frac{\mathbf{y}_{t+\Delta t}}{\beta \Delta t^2} - \mathbf{s}_t, \tag{13}$$

where β and γ are parameters equal to 1/4 and 1/2, respectively, while \mathbf{r}_t and \mathbf{s}_t are contributions from previous time step expressed as:

$$\mathbf{r}_{t} = \dot{\mathbf{y}}_{t} + \Delta t \left(1 - \gamma \right) \ddot{\mathbf{y}}_{t},\tag{14}$$

$$\mathbf{s}_{t} = \frac{\mathbf{y}_{t}}{\beta \Delta t^{2}} + \frac{\dot{\mathbf{y}}_{t}}{\beta \Delta t} + \left(\frac{1}{2\beta} - 1\right) \ddot{\mathbf{y}}_{t}.$$
 (15)

Substituting Equations (12) and (13) in (9) and (11) one leads to the discretized system:

$$\left(\frac{1}{\beta \Delta t^2} \mathbf{M} + \frac{\gamma}{\beta \Delta t} \mathbf{K}\right) \cdot \mathbf{y}_{t+\Delta t} - \mathbf{G} \cdot \mathbf{p}_{t+\Delta t} = \mathbf{f}_{t+\Delta t}^{ext} - \mathbf{K} \cdot \mathbf{r}_t + \gamma \Delta t \mathbf{K} \cdot \mathbf{s}_t + \mathbf{M} \cdot \mathbf{s}_t, \tag{16}$$

$$\left(\frac{\gamma}{\beta \Delta t} \mathbf{D} + \frac{1}{\beta \Delta t^2} \mathbf{C}_{PSPG}\right) \cdot \mathbf{y}_{t+\Delta t} + \mathbf{L}_{PSPG} \cdot \mathbf{p}_{t+\Delta t} = \mathbf{h}_{PSPG} - \mathbf{D} \cdot \mathbf{r}_t + \gamma \Delta t \mathbf{D} \cdot \mathbf{s}_t + \mathbf{C}_{PSPG} \cdot \mathbf{s}_t,$$
(17)

in which matrices C_{PSPG} , L_{PSPG} and vector h_{PSPG} come from PSPG stabilization, as one sees in Cremonesi et al. [16], Tezduyar and Osawa [24].

2.3 PFEM

The PFEM is a combination of FEM with particle methods concepts to allow the simulation of free surface flows which undergo large distortions and topological changes. All the physical properties eg. viscosity, density, are stored in particles instead of elements, making easy to build a new mesh without the need of transferring information from one mesh to another.

Since it is based on a Lagrangian description, the main difficulty becomes the maintenance of mesh quality throughout the analysis. For this reason, remesh is performed every time over the particles combined with a boundary identification technique to correctly draw the computational domain. The way we implemented PFEM can be summarized in the following steps (Figure 1):

- Discretize the fluid domain in a set of physical particles;
- Perform a Delaunay triangulation to generate a FEM mesh connecting the particles;
- Use the α -shape technique to erase too distorted elements and correctly identify the boundaries;

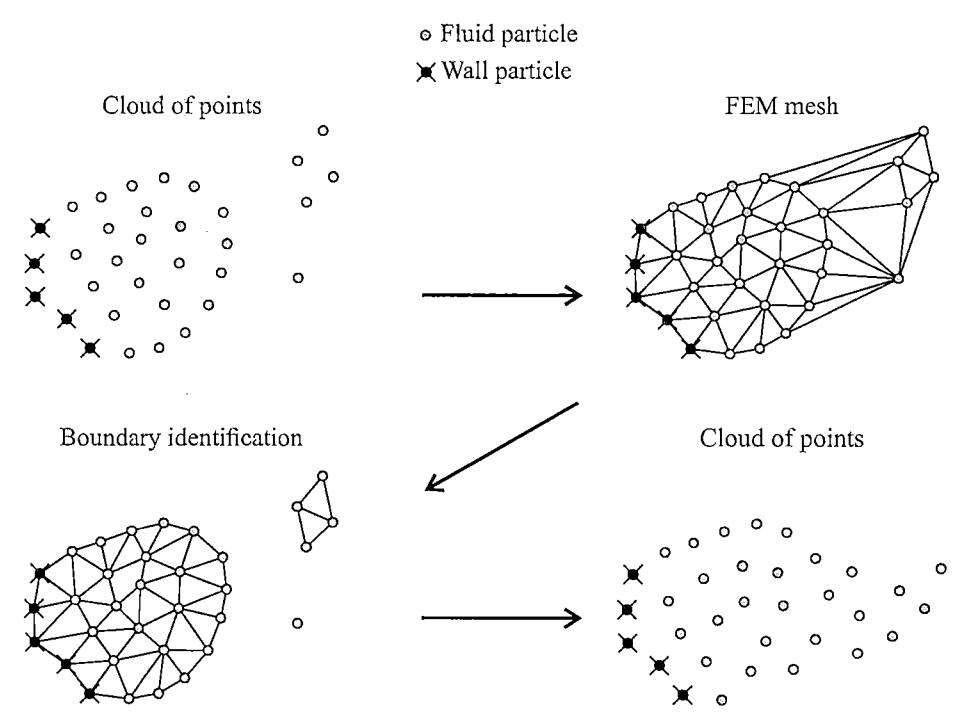


Figure 1. The basis of PFEM

- Solve governing equations for both particle current position and pressure using FEM;
- Erase the mesh and repeat the steps 2 to 4 until the last time step.

In this work the Delaunay triangulation is performed using the open source library "triangle", developed by Shewchuk [25]. The algorithm itself cannot prevent the creation of highly distorted elements and thus we combine it with the α -shape technique for both preserving mesh quality and to correctly identify the external boundaries.

Considering that h_e is the mesh size, taken to be equal to the minimum distance between two particles, the α -shape method consists on checking for every element if its circumradius r_e , computed as the radius of a circumscribed circle of the element, is less than h_e scaled by an arbitrary parameter α :

$$r_e < \alpha h_e. \tag{18}$$

Elements that fail to pass the test of Equation (18) are considered too much distorted and are removed. One can see that α plays a key role and needs to be set properly, as we can see in Figure 2. If its value is excessively high, no element will be erased and the boundaries will not be effectively identified. On the other hand, if α is too small, the condition will not hold for all elements and the result will be a cloud of isolated particles. A recommended value for α lies between 1.0 and 1.5, as stated by Idelsohn et al. [12], Franci [26] and many other authors.

3 Positional formulation applied to structural dynamic analysis

The equation that describes the solid motion is here solved using the positional finite element method, which is based on a Total Lagrangian description and uses the principle of stationary total energy to assemble the variational problem. An energy functional can be written globally as a sum of the internal strain energy, kinect energy, the potential energy due to external loads, and a dissipative energy:

$$\Pi = \int_{\Omega_0} \Psi(\mathbf{E}) d\Omega_0 + \int_{\Omega_0} \frac{1}{2} \rho_0 \dot{\mathbf{y}} \cdot \dot{\mathbf{y}} d\Omega_0 - \int_{\Gamma_0} \mathbf{t} \cdot \mathbf{y} d\Gamma_0 - \mathbf{p} \cdot \mathbf{y} + \mathcal{L}(\mathbf{y}), \qquad (19)$$

where Ψ represents the Helmholtz free-energy, y is the current position vector, t and p are surface tractions and concentrated loads, respectively, and \mathcal{L} is the dissipated energy which are not explicitly

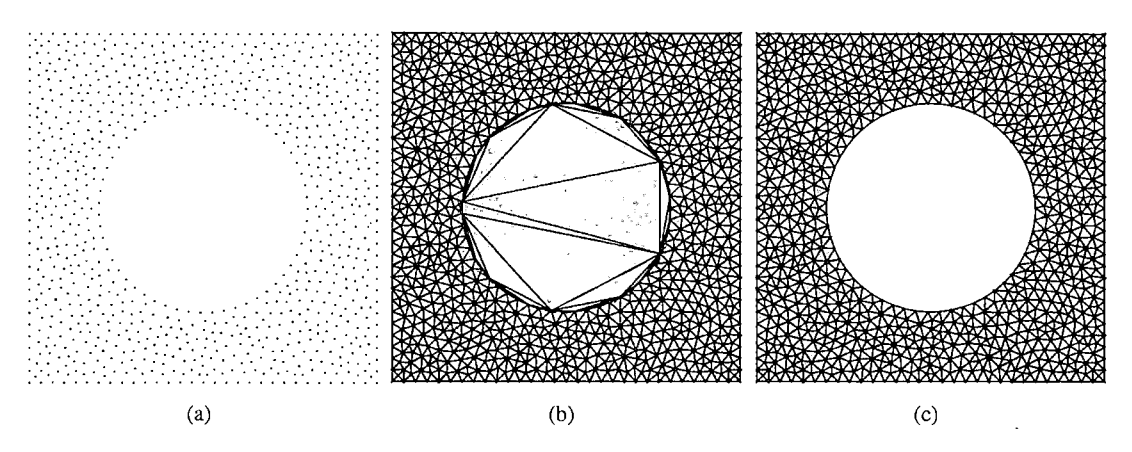


Figure 2. Role played by α parameter. (a) $\alpha = 0.1$, (b) $\alpha = 10.0$ and (c) $\alpha = 1.5$

known, however an expression can be obtained for its variation.

By applying the principle of stationary total energy, one obtains the dynamic equilibrium, which happens when:

$$\delta \Pi = 0. \tag{20}$$

The first variation can be numerically computed as the energy functional depends only on nodal positions. Performing some algebra manipulations and adopting Saint-Venant-Kirchhoff constitutive law one writes:

$$\int_{\Omega_0} \mathbf{S} : \frac{\partial \mathbf{E}}{\partial \mathbf{y}} \cdot \delta \mathbf{y} d\Omega_0 + \int_{\Omega_0} \rho_0 \ddot{\mathbf{y}} \cdot \delta \mathbf{y} d\Omega_0 - \int_{\Gamma_0} \mathbf{t} \cdot \delta \mathbf{y} d\Gamma_0 - \mathbf{f} \cdot \delta \mathbf{y} + \int_{\Omega_0} c\rho_0 \ddot{\mathbf{y}} \cdot \delta \mathbf{y} d\Omega_0, \tag{21}$$

where the last term refers to a Rayleigh-type damp scalled by a coefficient c, S and E are the second Piola-Kirchhoff stress tensor and Green strain tensor, respectively. For a complete development of the formulation, the readers should refer to Greco and Coda [19], Coda and Paccola [20], Siqueira and Coda [21].

The kinematics are described by approximating positions in the initial and current configurations in a classical FEM manner as:

$$\mathbf{x}^h = N_a \mathbf{x}_a \quad \text{and} \quad \mathbf{y}^h = N_a \mathbf{y}_a, \tag{22}$$

where x stands for the initial position vector. We use an isoparametric triangular element with cubic approximation to discretize the domain. The motion function \mathcal{X} is then written based on a composition of the mapped positions as:

$$\mathcal{X} = \mathbf{y} \circ \mathbf{x}^{-1}. \tag{23}$$

The Green strain can be numerically computed through the deformation gradient, so from Equation (23) one writes:

$$\mathbf{A} = \nabla \mathcal{X} = \mathbf{A}^1 \circ \left(\mathbf{A}^0\right)^{-1},\tag{24}$$

where A^1 and A^0 are numerical gradients related to the derivatives regarding the parametric coordinates ξ of y^h and x^h , computed as:

$$\mathbf{A}^{1} = \frac{\partial \mathbf{y}}{\partial \boldsymbol{\xi}} \quad ; \quad \mathbf{A}^{0} = \frac{\partial \mathbf{x}}{\partial \boldsymbol{\xi}}, \tag{25}$$

and finally the Green strain tensor is written as:

$$\mathbf{E} = \frac{1}{2} \left(\mathbf{A}^t \mathbf{A} - \mathbf{I} \right), \tag{26}$$

with I stading for the identity tensor. Using the Saint-Venant-Kirchhoff model one calculates second Piola-Kirchhoff stress tensor from:

$$S = C : E, \tag{27}$$

in which C is the fourth order constitutive tensor that can be found in elasticity books (Holzapfel [27]). Reminding the arbitratiness of $\delta \mathbf{v}$ in Equation (21), one writes the non-linear system in its matricial

Reminding the arbitratiness of δy in Equation (21), one writes the non-linear system in its matricial form:

$$\mathbf{f}^{int} + \mathbf{M} \cdot \ddot{\mathbf{y}} + \mathbf{C} \cdot \dot{\mathbf{y}} - \mathbf{f}^{ext} = 0, \tag{28}$$

where \mathbf{f}^{int} and \mathbf{f}^{ext} are the internal and external force vectors respectively, \mathbf{M} is the mass matrix and \mathbf{C} refers to the damp matrix computed as $\mathbf{C} = c\mathbf{M}$. Equation (28) is a nonlinear system that is solved applying the Newton Raphson technique. The time marching procedure is achieved using again the Newmark- β , leading to the discretized system:

$$\mathbf{f}_{t+\Delta t}^{int} + \left(\frac{1}{\beta \Delta t^2} \mathbf{M} + \frac{\gamma}{\beta \Delta t} \mathbf{C}\right) \cdot \mathbf{y}_{t+\Delta t} = \mathbf{f}_{t+\Delta t}^{ext} + \mathbf{M} \cdot \mathbf{s}_t - \mathbf{C} \cdot \mathbf{r}_t + \gamma \Delta t \mathbf{C} \cdot \mathbf{s}_t.$$
 (29)

4 Coupling algorithm

Let consider Ω_f and Ω_s the domains occupied by a fluid and a solid, respectively, at a time t. The fluid-structure interface Γ_{fs} is then defined as the intersection between both domains, so that $\Gamma_{fs} = \Omega_f \cap \Omega_s$. The fluid and structural problems are coupled through the following continuity conditions:

$$\mathbf{x}_f = \mathbf{x}_s \quad \text{on } \Gamma_{fs},\tag{30}$$

$$\sigma_f \dot{\mathbf{n}}_f = -\sigma_s \mathbf{n}_s \quad \text{on } \Gamma_{fs},$$
 (31)

where x is the position vector, σ is the Cauchy stress and n is the normal vector to the interface. The coupling in this work is performed based on a Dirichlet-Neumann approach, where a block-iterative scheme is used to impose the interface conditions. Within the iterative process, the following steps are performed until a converged solution is reached: a) solve fluid problem for surface tractions; b) transfer surface tractions to the solid as Neumann conditions; c) solve structural problem for updated interface position and d) prescribe the new interface position in the fluid model as Dirichlet condition.

Since in this work the problems are not limited to the case where the structure is immersed in the fluid, the contact between them must be identified at every time step. For that reason, a set of ficticious particles, named by Cremonesi et al. [16] as ghost particles, is created in the fluid domain (Figure 3(a)). Each one of these ghost particles is placed superposed to the structure nodes that lie on the fluid-structure interface in a way that, when a fluid particle comes close to the solid boundary, the α -shape method automatically detects the contact. As we use an α parameter globally, the structure mesh must has a similar refinement as the initial particles distribution of the fluid domain. Then we proceed by performing the Delaunay triangulation to generate fluid mesh according to Figure 3(b), followed by applying the α -shape technique to erase distorted elements and to identify the boundaries (Figure 3(c)). At this point, we say that the domains are in contact if there is at least one fluid element which has a ghost particle as one of its nodes. If that is the case, we perform the coupled analysis (Figure 3(c)), otherwise, the domains are analysed separately as depicted in Figure 3(e).

5 Examples

We verify the developed formulation for three different cases in this section. Firstly, we test our fluid and solid codes separately, and then we solve a coupled problem using the approach described in Section 4.

5.1 Non-linear dynamic response of a clamped beam

In order to attest the robustness of the positional formulation when applied to non-linear dynamic analises, we simulate a clamped beam subjected to a central point load under large displacements from

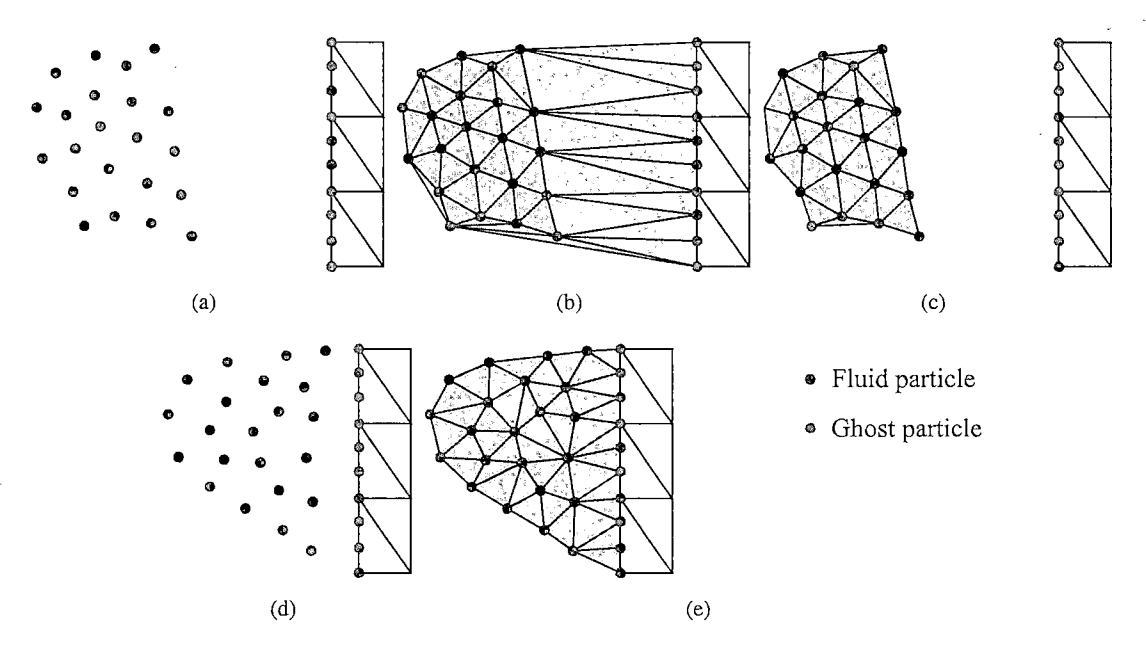


Figure 3. Fluid-structure contact detection

Mondkar and Powell [28]. The geometry and boundary conditions are depicted in Figure 4, with L=20.0 m, h=0.125 m, unitary thickness, P=640 N and the material properties adopted are $E=30.0 \text{x} 10^6$ Pa , $\nu=0.0$ and $\rho=2.537.10^{-4}$ kg/m³, where the units were adapted to the SI.

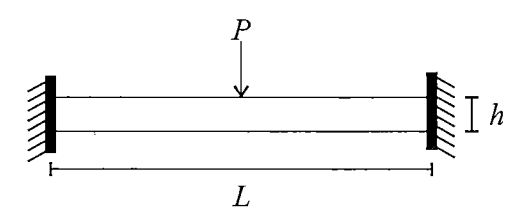


Figure 4. Non-linear dynamic response of a clamped beam. Initial geometry

The domain was discretized with 20 elements and 124 nodes, and a time step $\Delta t = 0.00002$ s was employed. One can notice from a linear analysis that this problem presents large displacements, thus we show in Figure 5 the amplitude of vibration in the center of the span for the linear and non-linear cases. Due to membrane effects, one expects a stiffening behaviour which highly affects the solution, increasing the frequency and shortening the period of vibration when compared to the linear analysis. Also, one sees that our results agree well with reference.

5.2 Dam collapse

This example is a benchmark in computational fluid dynamics and consists on the collapse of a dam initially at rest, for which some experimental and numerical data are available in Koshizuka and Oka [29]. The problem geometry can be seen in Figure 6, where stick conditions were applied on the walls, L=0.146 m, gravity acceleration g=9.81 m/s² and the fluid physical properties are $\mu=0.001$ Pa.s and $\rho=1000.0$ kg/m³.

The analysis is performed using a initial particle distribution with a characteristic length $h_e=3.7$ mm and 4440 particles. A time step $\Delta t=0.001$ s was employed and the α parameter was set to 1.5. In Figure 7 a qualitatively comparison of the free surface shape between our results and the ones from Koshizuka and Oka [29] is presented. One can observe that the results are qualitatively similar to the references, especially for values of t<0.6 s when fluid does not present a significant amount of particles which have detached from the main domain and spilled out of the tank. Given the complexity of

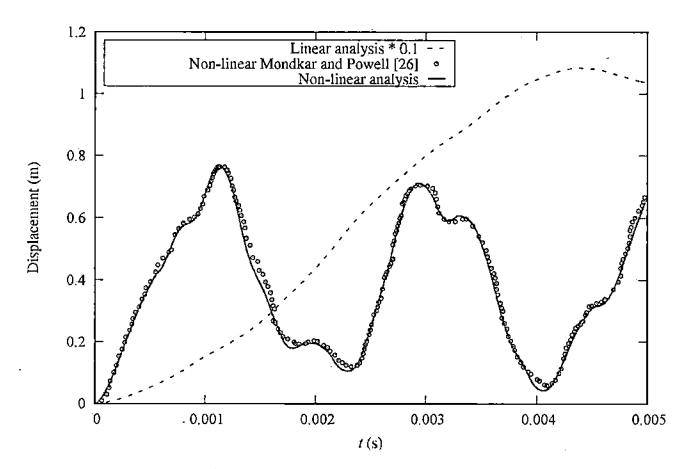


Figure 5. Non-linear dynamic response of a clamped beam. Comparison of linear and non-linear dynamic response

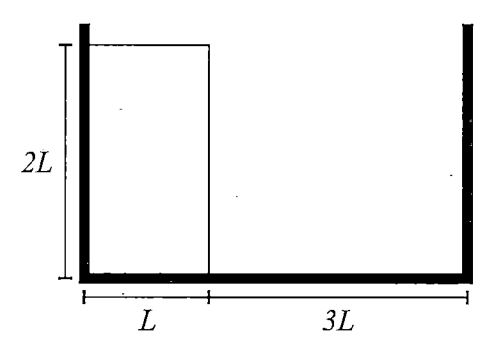


Figure 6. Dam collapse. Initial geometry

this kind of problem, we achieved satisfactory results. Figure 8 shows the velocity and pressure fields at different instants, where a smooth pressure distribution can be seen, ensuring the effectiveness of PSPG in stabilizing the formulation.

5.3 Water tank with highly flexible wall

A case involving a water tank with a highly flexible wall is studied in order to test our coupling technique. Firstly proposed by Zhu and Scott [30], the geometry is described in Figure 9, where L=0.1 m, H=0.08 m, w=0.012 m, the left and bottom walls are non-slip walls and at the right we have a flexible beam subjected to a hidrostatic pressure load. The beam has an elastic modulus, density and poisson equal to $E=1.0 \times 10^6$ Pa, $\rho_s=2500.0$ kg/m³, $\nu=0.0$, respectively, and no damp was considered, while the fluid properties are viscosity $\mu=0.1$ Pa.s, density $\rho_f=1000.0$ kg/m³.

The water pressure causes the beam to deflect, which in turn generates a sloshing wave in the reservoir, thus making it a coupled problem. We discretize the structure through a non-regular mesh with 46 elements and 244 nodes, resulting in a mesh size $h_e=3.33$ mm. To ensure the same characteristic length to the fluid discretization, we use 1200 particles and $\alpha=1.5$. A fixed time step $\Delta t=0.01$ s was employed for both domains and the gravity force acts downwards. Figure 10 shows the beam tip deflection and the pressure evolution at the bottom of the tank, while in Figure 11 the deformed shape is plotted for different instants. One notice that using the Dirichlet-Neumann approach combined with the ghost particles technique is a practical way to obtain a good solution. Also, the results were obtained with only 2 iterations, and in fact, for this kind of problem a weak-coupling scheme would be sufficient as the solid/fluid density ratio is not equal to 1, thus the problem does not present added-mass effect.

6 Conclusion

In this paper, we develop a particle-position based PFEM formulation for free surface flows and FSI problems. By using a Lagrangian description for representing both solid and fluid motion, coupling is straightforward. A technique based on ghost particles is employed in order to model fluid/solid contact with aid of α -shape method, which revealed to be very robust, leading to good results. Regarding the structural problem solver, the positional formulation reveals to be a simple but effective tool to analyse structures under large displacements, suitable for FSI problems.

The PFEM also demonstrates to be a very versatile strategy to handle very large domain distortions, topological changes and domain fragmentation, ideal to be used in free surface flow analyses. Smooth velocity and pressure distributions are obtained thanks to the PSPG stabilization technique, which effectively circumvents the LBB condition and lead to a stabilized formulation.

Finally, the strong-coupling technique used in this work has shown to be a simple way to simulate FSI problems in a partitioned way. Alternatively, as fluid and solid solvers have nodal positions as main variables, it becomes straightforward to implement a monolithic strategy for solving coupled problems, and the authors are considering it for future works.

Acknowledgements

The authors would like to thank the financial support given by the Coordination for the Improvement of Higher Education Personnel (CAPES), finance code 001, and by the Brazilian National Council for Research and Technological Development (CNPq) - grants 310482/2016-0 and 141804/2018-1.

References

- [1] Donea, J., Giuliani, S., & Halleux, J. P., 1982. An arbitrary lagrangian-eulerian finite element method for transient dynamic fluid-structure interactions. *Computer Methods in Applied Mechanics and Engineering*, vol. 33, pp. 689–723.
- [2] Fernandes, J. W. D., Coda, H. B., & Sanches, R. A. K., 2019. ALE incompressible fluid-shell coupling based on a higher-order auxiliary mesh and positional shell finite element. *Computational Mechanics*, vol. 63, n. 3, pp. 555–569.
- [3] Hughes, T. J., Liu, W. K., & Zimmermann, T. K., 1981. Lagrangian-Eulerian finite element formulation for incompressible viscous flows. *Computer Methods in Applied Mechanics and Engineering*, vol. 29, n. 3, pp. 329–349.
- [4] Del Pin, F., Idelsohn, S., Oñate, E., & Aubry, R., 2007. The ALE/Lagrangian particle finite element method: a new approach to computation of free-surface flows and fluid-object interactions. *Computers & Fluids*, vol. 36, n. 1, pp. 27–38.
- [5] Takizawa, K. & Tezduyar, T. E., 2011. Multiscale Space-Time fluid-structure interaction techniques. *Computational Mechanics*, vol. 48, n. 3, pp. 247–267.
- [6] Masud, A. & Hughes, T. J. R., 1997. A Space-time Galerkin/Least-Squares finite element formulation of the Navier-Stokes equations for moving momain problems. *Computer Methods in Applied Mechanics and Engineering*, vol. 146, pp. 91–126.
- [7] Hübner, B., Walhorn, E., & Dinkler, D., 2004. A monolithic approach to fluid-structure interaction using Space-Time finite elements. *Computer methods in applied mechanics and engineering*, vol. 193, n. 23-26, pp. 2087–2104.
- [8] Peskin, C. S., 2002. The immersed boundary method. Acta numerica, vol. 11, pp. 479–517.

- [9] Mittal, R. & Iaccarino, G., 2005. Immersed boundary methods. *Annual Review of Fluid Mechanics*, vol. 37, pp. 239–261.
- [10] Gingold, R. A. & Monaghan, J. J., 1977. Smoothed particle hydrodynamics: theory and application to non-spherical stars. *Monthly notices of the royal astronomical society*, vol. 181, n. 3, pp. 375–389.
- [11] Idelsohn, S. R., Oñate, E., & Pin, F. D., 2004. The particle finite element method: a powerful tool to solve incompressible flows with free-surfaces and breaking waves. *International Journal for Numerical Methods in Engineering*, vol. 61, n. 7, pp. 964–989.
- [12] Idelsohn, S. R., Oñate, E., Pin, F. D., & Calvo, N., 2006. Fluid-structure interaction using the particle finite element method. *Computer Methods in Applied Mechanics and Engineering*, vol. 195, n. 17-18, pp. 2100–2123.
- [13] Idelsohn, S. R., Marti, J., Limache, A., & Oñate, E., 2008. Unified Lagrangian formulation for elastic solids and incompressible fluids: application to fluid-structure interaction problems via the PFEM. Computer Methods in Applied Mechanics and Engineering, vol. 197, n. 19-20, pp. 1762–1776.
- [14] Oñate, E., Idelsohn, S. R., Del Pin, F., & Aubry, R., 2004. The particle finite element method-an overview. *International Journal of Computational Methods*, vol. 1, n. 02, pp. 267–307.
- [15] Carbonell, J. M., Oñate, E., & Suárez, B., 2009. Modeling of ground excavation with the particle finite-element method. *Journal of engineering mechanics*, vol. 136, n. 4, pp. 455–463.
- [16] Cremonesi, M., Frangi, A., & Perego, U., 2010. A Lagrangian finite element approach for the analysis of fluid-structure interaction problems. *International Journal for Numerical Methods in Engineering*, vol. 84, n. 5, pp. 610–630.
- [17] Cerquaglia, M. L., Deliége, G., Boman, R., Terrapon, V., & Ponthot, J.-P., 2017. Free-slip boundary conditions for simulating free-surface incompressible flows through the particle finite element method. *International Journal for Numerical Methods in Engineering*, vol. 110, n. 10, pp. 921–946.
- [18] Edelsbrunner, H. & Mücke, E. P., 1994. Three-dimensional alpha shapes. *ACM Transactions on Graphics (TOG)*, vol. 13, n. 1, pp. 43–72.
- [19] Greco, M. & Coda, H. B., 2004. A simple and precise FEM formulation for large deflection 2d frame analysis based on position description. *Computer Methods in Applied Mechanics and Engineering*, vol. 193.
- [20] Coda, H. B. & Paccola, R. R., 2007. An alternative positional FEM formulation for geometrically non-linear analysis of shells: Curved triangular isoparametric elements. *Computional Mechanics*, vol. 40, n. 1, pp. 185–200.
- [21] Siqueira, T. M. & Coda, H. B., 2019. Flexible actuator finite element applied to spatial mechanisms by a finite deformation dynamic formulation. *Computational Mechanics*, vol. 1, pp. 1–19.
- [22] Sanches, R. A. K. & Coda, H. B., 2014. On fluid-shell coupling using an arbitrary lagrangian-eulerian fluid solver coupled to a positional Lagrangian shell solver. *Applied Mathematical Modelling*, vol. 38, pp. 3401–3418.
- [23] Tezduyar, T. E., Mittal, S., Ray, S. E., & Shih, R., 1992. Incompressible flow computations with stabilized bilinear and linear equal-order-interpolation velocity-pressure elements. *Computer Methods in Applied Mechanics and Engineering*, vol. 95, n. 2, pp. 221–242.
- [24] Tezduyar, T. E. & Osawa, Y., 2000. Finite element stabilization parameters computed from element matrices and vectors. *Computer Methods in Applied Mechanics and Engineering*, vol. 190, n. 3-4, pp. 411–430.

- [25] Shewchuk, J. R., 2002. Delaunay refinement algorithms for triangular mesh generation. *Computational geometry*, vol. 22, n. 1-3, pp. 21–74.
- [26] Franci, A., 2016. Unified Lagrangian formulation for fluid and solid mechanics, fluid-structure interaction and coupled thermal problems using the PFEM. Springer.
- [27] Holzapfel, G. A., 2002. Nonlinear solid mechanics: a continuum approach for engineering science. *Meccanica*, vol. 37, n. 4, pp. 489–490.
- [28] Mondkar, D. P. & Powell, G. H., 1977. Finite element analysis of non-linear static and dynamic response. *International journal for numerical methods in engineering*, vol. 11, n. 3, pp. 499–520.
- [29] Koshizuka, S. & Oka, Y., 1996. Moving-particle semi-implicit method for fragmentation of incompressible fluid. *Nuclear science and engineering*, vol. 123, n. 3, pp. 421–434.
- [30] Zhu, M. & Scott, M. H., 2017. Direct differentiation of the quasi-incompressible fluid formulation of fluid-structure interaction using the PFEM. *Computational Particle Mechanics*, vol. 4, n. 3, pp. 307–319.

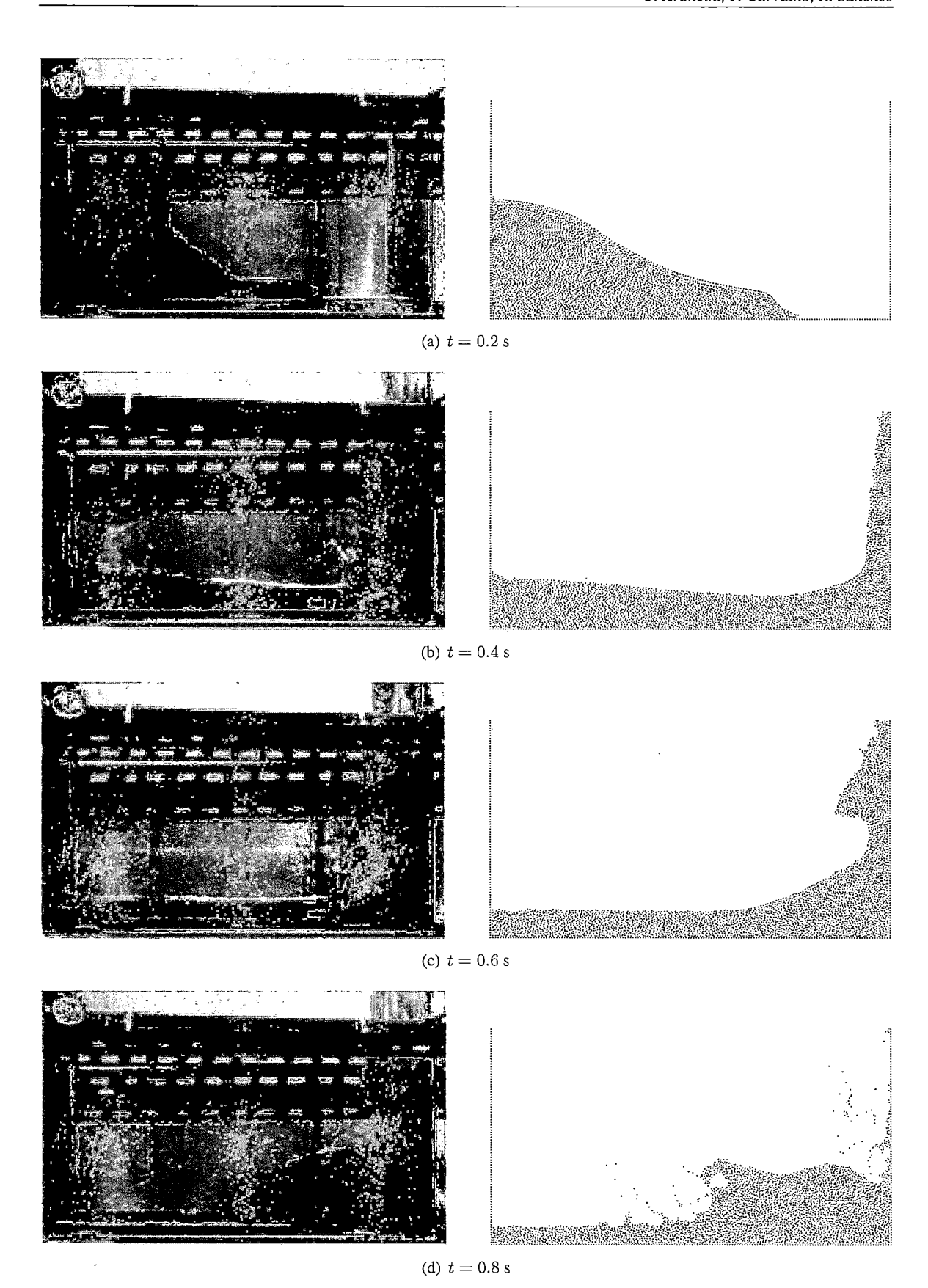


Figure 7. Dam collapse. Free surface shape. Koshizuka and Oka [29] experimental (left) and proposed formulation (right)

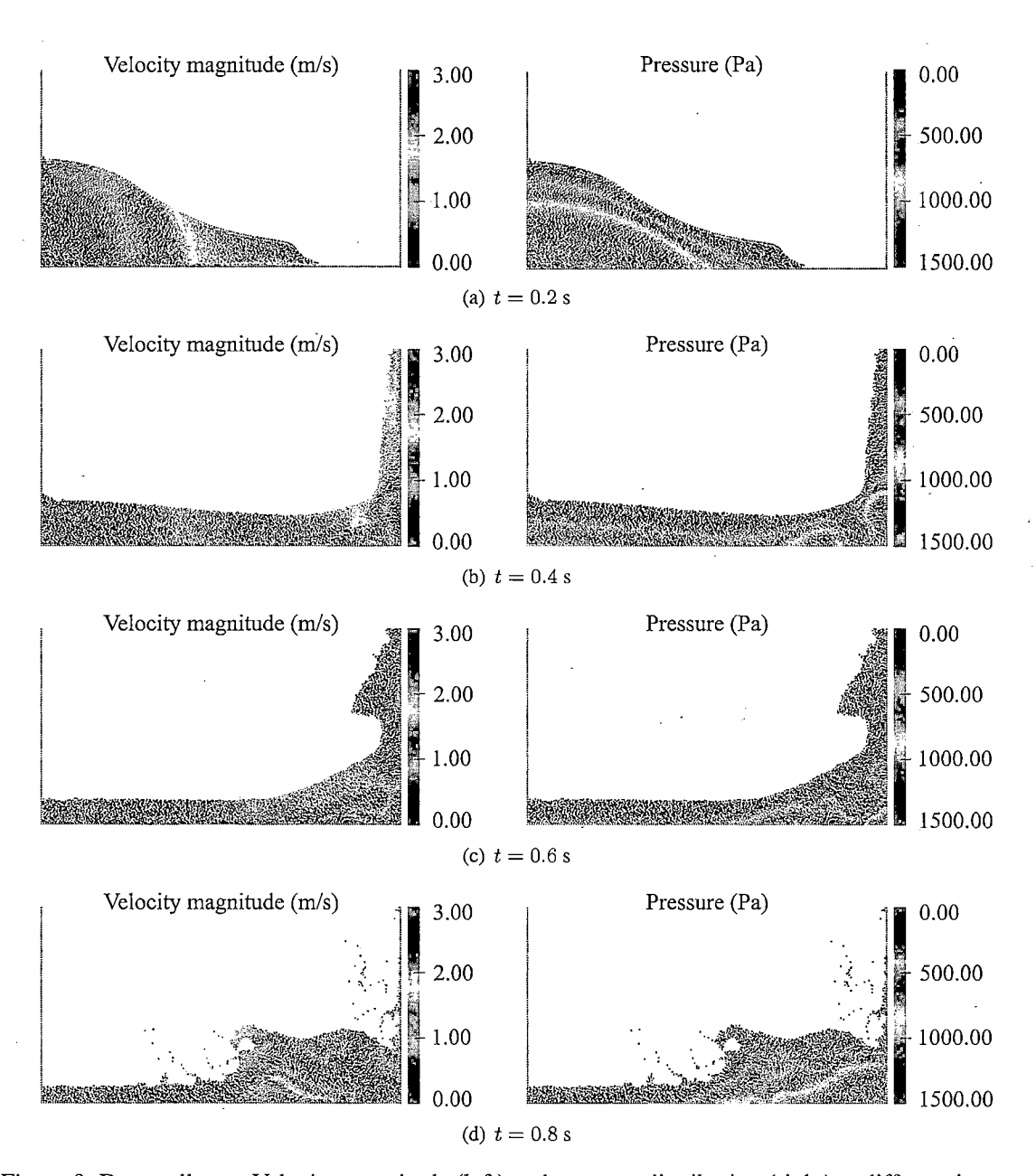


Figure 8. Dam collapse. Velocity magnitude (left) and pressure distribution (right) at different instants

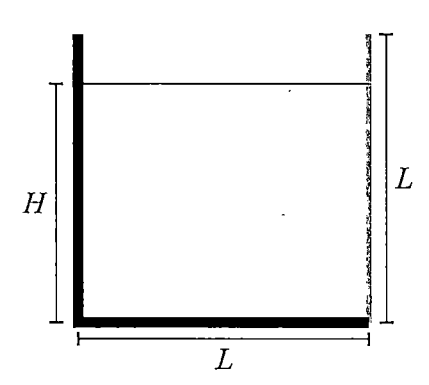


Figure 9. Water tank with higly flexible wall. Initial geometry

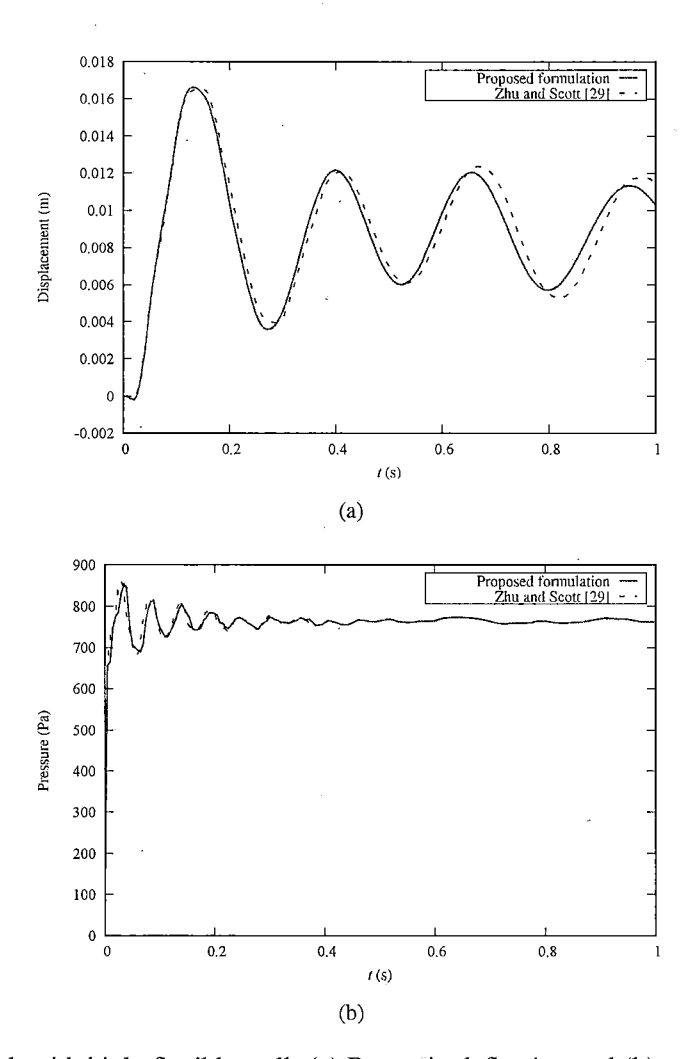


Figure 10. Water tank with higly flexible wall. (a) Beam tip deflection and (b) pressure evolution at the bottom of reservoir

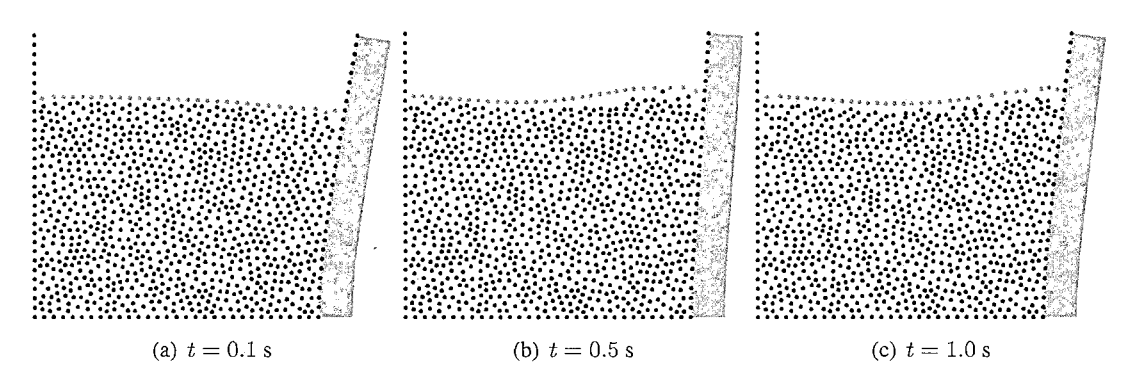


Figure 11. Water tank with higly flexible wall. Deformed shape

